

Data Augmentation for Deep Receivers

Tomer Raviv and Nir Shlezinger

Abstract

Deep neural networks (DNNs) allow digital receivers to learn to operate in complex environments. To do so, DNNs should preferably be trained using large labeled data sets with a similar statistical relationship as the one under which they are to infer. For DNN-aided receivers, obtaining labeled data conventionally involves pilot signalling at the cost of reduced spectral efficiency, typically resulting in access to limited data sets. In this paper, we study how one can enrich a small set of labeled pilots data into a larger data set for training deep receivers. Motivated by the widespread use of data augmentation techniques for enriching visual and text data, we propose dedicated augmentation schemes that exploits the characteristics of digital communication data. We identify the key considerations in data augmentations for deep receivers as the need for domain orientation, class (constellation) diversity, and low complexity. Following these guidelines, we devise three complementing augmentations that exploit the geometric properties of digital constellations. Our combined augmentation approach builds on the merits of these different augmentations to synthesize reliable data from a momentary channel distribution, to be used for training deep receivers. Furthermore, we exploit previous channel realizations to increase the reliability of the augmented samples. The superiority of our approach is numerically evaluated for training several deep receiver architectures in different channel conditions. We consider both linear and non-linear synthetic channels, as well as the COST 2100 channel generator, for both single-input single-output and multiple-input multiple-output scenarios. We show that our combined augmentations approach allows DNN-aided receivers to achieve gains of up to 1 dB in bit error rate and of up to $\times 3$ in spectral efficiency, compared to regular non-augmented training. Moreover, we demonstrate that our augmentations benefit training even as the number of pilots increases, and perform an ablation study on the different augmentations, which shows that the combined approach surpasses each individual augmentation technique.

I. INTRODUCTION

The emergence of deep learning has notably impacted numerous applications in various disciplines. The ability of deep neural networks (DNNs) to learn to efficiently carry out complex tasks from data has spurred a growing interest in their usage for receiver design in digital

Parts of this work were presented at the 2022 IEEE Workshop on Signal Processing Advances in Wireless Communications (SPAWC) as the paper [1]. This project has received funding from the Israeli 5G-WIN consortium. The authors are with the School of ECE, Ben-Gurion University of the Negev, Beer-Sheva, Israel (e-mail: tomerraviv95@gmail.com, nirshl@bgu.ac.il).

communications [2]–[5]. While traditional receiver algorithms are channel-model-based, relying on mathematical modeling of the signal transmission, propagation, and reception, DNN-based receivers have the potential to operate efficiently in model-deficient scenarios where the channel model is unknown, highly complex, or difficult to optimize for [5], and can thus greatly contribute to meeting the constantly growing requirements of wireless systems in terms of throughput, coverage, and robustness [6]. Generally, deep learning can be integrated with receiver design either by using conventional black-box DNN architectures trained end-to-end; or by leveraging model-based solutions [7]–[10], whereby specific blocks of a receiver’s architecture are replaced by neural networks, e.g., via deep unfolding [4].

While deep learning thrives in domains such as computer vision and natural language processing, many challenges still limit its widespread applicability in digital communications. One of these challenges arises from the fact that DNNs rely on (typically labeled) data sets to learn their mappings, and are thus usually applied when the function being learned is stationary for a long period of time, such that one can collect sufficient data for learning. For example, data sets for machine translation tasks, which are nowadays dominated by deep learning systems, are usually composed of a sentence in an origin language, and its respective translation in a destination language, which do not change much with time. One can thus collect a large volume of such pairs for training, obtaining a huge data set for the task at hand [11].

In contrast, the operation of digital receivers is rarely stationary, as communication channels (and thus the data distribution and in turn the system task) change considerably over time. Moreover, DNNs are highly-parameterized models, and their training requires massive data sets. In digital receivers, labeled data corresponding to the current channel is often obtained from pilots, whose transmission degrades the spectral efficiency. Thus, deployed digital receivers are likely to have access to small labeled data sets corresponding to the current task, hardly in the scale needed to train DNNs. Consequently, a core challenge associated with the usage of DNN-aided receivers stems from the need to aggregate sufficient task-specific data, i.e., data corresponding to the instantaneous setting where the receiver is required to operate.

Various strategies have been proposed to facilitate the application of DNNs-aided receivers with limited data sets. The first approach trains with data obtained from simulations and past measurements, while using the limited data corresponding to the instantaneous channel to estimate some missing parameters, e.g., a channel matrix. These parameters are then used by the network, either as an input [12], [13] or as part of some internal processing [14]–[20]. This

involves imposing a relatively simple model on the channel, typically a linear Gaussian model, which limits their suitability in the presence of complex channel models.

An alternative approach designs receivers with compact task-specific DNNs such that they can be trained with relatively small data sets, by integrating them into classic receiver processing via model-based deep learning techniques [7], [8], see, e.g., [21]–[25]. These hybrid model-based/data-driven receivers build on existing communication models and incorporate deep learning into their design. The resulting architectures are agnostic to the channel model and its parameters, imitating the operation of a detection algorithm with no channel knowledge. Although these DNN-aided receivers are compact in terms of trainable parameters, the amount of data required in training is still likely to be larger than the amount corresponding to the instantaneous channel one can typically obtain in real-time.

A third approach aims to optimize the training algorithm itself, rather than the architecture, facilitating rapid convergence of the training procedure with limited data. Optimizing the hyperparameters that govern the optimization process, e.g., the initialization of the trainable weights, can intuitively be seen as a method to share data from different time steps, increasing the effective labeled data sets. This can be achieved by leveraging data corresponding to past channel realizations in order to tune the optimization hyperparameters via Bayesian optimization techniques [26]; model-agnostic meta-learning [27]–[29]; and predictive meta-learning for learning transition patterns in time-varying channels [30], [31].

The aforementioned strategies focus on either the architecture or the training algorithm. A complementary approach to cope with limited data sets, which can be combined with any of the above techniques, is to generate more data at the receiver. Current techniques for obtaining additional labeled data in wireless communications aim at assigning labels to channel outputs not associated with pilots by exploiting the presence of channel coding for self-supervision [22], [23], [32]–[34] or by using active learning techniques [35], [36]. However, these approaches cannot synthesize more data than the block length (typically generating much less [36]), and the resulting data set may be too small for training.

A common practice in the deep learning literature is to synthesize data samples via *data augmentation*. Data augmentation is a set of techniques that enrich a trainable model with new unseen synthetic data, where each technique builds on partial knowledge of the data characteristics [37]–[40], typically exploiting some underlying translation invariance. For instance, in image classification, one can use a labeled image to generate multiple different images with the

same label by, e.g., rotating or clipping it [37], [38]. While data augmentation is a widely used deep learning technique, it is highly geared towards image and language data. This motivates the study of augmentation techniques for enriching data in digital communications, as means to facilitate the training of DNN-aided receivers with limited labeled data sets.

Main Contributions

In this paper we propose a data augmentation framework for DNN-aided receivers. Our proposed method introduces a set of data synthesis techniques which exploit expected structures of digital communication symbols and their corresponding channel outputs to enrich a small labeled data set with many reliable samples. The resulting enriched data can then be used for training, so as to reduce the error rate obtained by the receiver, and specifically the epistemic uncertainty that exists due to limitations of available training data [41]. Our main contributions are summarized as follows:

- **Proposed framework:** We formulate a communication-directed data augmentations framework, which embodies the specific characteristics of the digital communication data used for training DNN-aided receivers.
- **Communications-tailored augmentations:** We propose several augmentations that exploit innate traits of digital constellations. We exploit both expected symmetries in channel outputs as well as identified communication-specific translation invariance properties to generate new synthetic samples for training. Our proposed augmentation techniques are complementary of each other, and are combined into a unified method.
- **Adaptive augmentations for time-varying channels:** We extend our augmentation techniques to temporally adapt for deep receivers operating in block-fading channels. This allows leveraging past channels to generate additional synthetic data to be used for online training in time-varying conditions.
- **Extensive experimentation:** We extensively evaluate the proposed training scheme for training various DNN-aided receiver architectures. We consider different channel profiles for both multipath single-input single-output (SISO) channels as well as memoryless multiple-input multiple-output (MIMO) systems. We demonstrate consistent benefits by using our approach, which amount to gains of up to 1 dB in bit error rate, and of up to $\times 3$ in spectral efficiency, compared with non-augmented training. Moreover, we show that our augmentations benefit training even as the number of pilots increases, and perform an

ablation study on the different augmentations, which shows that combining the augmentation techniques benefits upon using each of the individual methods.

The rest of this paper is organized as follows: Section II details the system model and the operation of DNN-aided receivers. Section III formulates the framework and presents the augmentation techniques for static channels, where a single small data set corresponding to a specific channel realization is to be synthetically enriched for training. Section IV extends the augmentation techniques to dynamic communication setups, accounting for continuous variations in block-fading channels. Experimental results and concluding remarks are detailed in Section V and Section VI, respectively.

Throughout the paper, we use boldface letters for vectors, e.g., \mathbf{x} ; $(\mathbf{x})_i$ denotes the i th element of \mathbf{x} . Upper-cased boldface letters denote matrices, e.g., \mathbf{X} , with \mathbf{I}_n being the $n \times n$ identity matrix. Calligraphic letters, such as \mathcal{X} , are used for sets, with $|\mathcal{X}|$ being the cardinality of \mathcal{X} . We denote by \mathcal{R} and \mathcal{C} the sets of real and complex numbers, respectively, while $\mathcal{N}(\cdot, \cdot)$ is the Gaussian distribution. The operation $(\cdot)^H$ stands for the conjugate transpose operation.

II. SYSTEM MODEL

In the section, present the system model. To that aim, we first describe the communication model in Subsection II-A. Then, we discuss the receiver processing and the considered problem formulation of data augmentation for DNN-aided receivers in Subsections II-B and II-C, respectively.

A. Communication Model

We consider a digital communication system in discrete-time. Let $\mathbf{s}_i \in \mathcal{S}$ be a symbol transmitted from constellation \mathcal{S} (with its size denoted $|\mathcal{S}|$) at the i th time instance within a block of B^{tran} symbols, i.e., $i \in \{1, 2, \dots, B^{\text{tran}}\} = \mathcal{B}$. The transmitted symbols block $\mathbf{s}^{\text{tran}} := \{\mathbf{s}_i\}_{i \in \mathcal{B}}$ is divided into B^{pilot} pilots that are known to the receiver and appear first, denoted $\mathbf{s}^{\text{pilot}}$, and $B^{\text{info}} = B^{\text{tran}} - B^{\text{pilot}}$ information symbols, denoted \mathbf{s}^{info} , that contain the digital message conveyed to the receiver. The channel output at time instance i is denoted by \mathbf{y}_i , which takes values in the set \mathcal{Y} , and the received block is $\mathbf{y}^{\text{rec}} := \{\mathbf{y}_i\}_{i \in \mathcal{B}}$. Similarly as the channel input, the channel output can be separated by the receiver into its pilot and information parts denoted $\mathbf{y}^{\text{pilot}}$ and \mathbf{y}^{info} , respectively. We assume that the channel, i.e., the mapping from \mathbf{s} into \mathbf{y} , is constant within the block of B^{tran} channel uses, which thus corresponds to the coherence duration of the channel.

Channel Models: While the above channel model is generic, we focus mostly on the common setting of communication over casual finite-memory channels. Such models accommodate a broad range of communication scenarios, including the following settings which are considered in our experimental study:

- 1) *Finite-Memory SISO Channels:* In multipath SISO channels, the channel output \mathbf{y}_i (which is scalar and thus written as y_i) is given by a stochastic function of the last $K > 0$ transmitted symbols, which can be stacked into the $K \times 1$ vector \mathbf{s}_i , where K is the memory length. Letting M be the alphabet size, the number of different constellation combinations that \mathbf{s}_i can represent is $|\mathcal{S}| = M^K$. Independence between different blocks is obtained by setting a guard interval of at least $K - 1$ time instances prior to the beginning of the block.
- 2) *Flat MIMO Channels:* Another channel of interest is the memoryless uplink MIMO channel, where K single-antenna transmitters (users) communicate with a receiver equipped with N antennas. Again letting M be the alphabet size, the channel input is the $K \times 1$ vector \mathbf{s}_i , which can take $|\mathcal{S}| = M^K$ different values, while the channel output is an $N \times 1$ vector.

Based on the above examples, we henceforth consider the symbol space \mathcal{S} to be comprised of $K \times 1$, i.e., $\mathcal{S} \subset \mathcal{C}^K$, and the channel outputs \mathbf{y}_i to be $N \times 1$ vectors, for some fixed $N, K > 0$.

B. Receiver Operation

The receiver processing is aided by a DNN which relies on labeled data to learn its mapping. In particular, the receiver recovers the information symbols from \mathbf{y}^{info} using a DNN-aided detection mapping, which yields the estimate $\hat{\mathbf{s}}(\mathbf{y}^{\text{info}}; \boldsymbol{\varphi})$, where $\boldsymbol{\varphi}$ are the parameters of the DNN. The parameters $\boldsymbol{\varphi}$ are obtained by training, using the available labeled data, denoted by \mathcal{Q}^* , which corresponds to the underlying channel and is comprised of pairs of channel outputs \mathbf{y}_i and their corresponding symbol vectors \mathbf{s}_i . The training module follows a (stochastic) gradient-based optimization with empirical loss measure $\mathcal{L}_{\mathcal{Q}^*}$, e.g., I_{sgd} iterations of the form

$$\boldsymbol{\varphi}^{(t+1)} = \boldsymbol{\varphi}^{(t)} - \eta \hat{\nabla}_{\boldsymbol{\varphi}} \mathcal{L}_{\mathcal{Q}^*}(\boldsymbol{\varphi}^{(t)}), \quad (1)$$

where $\eta > 0$ is the learning rate and $\hat{\nabla}_{\boldsymbol{\varphi}} \mathcal{L}$ is a stochastic approximation of the gradient of the empirical loss with respect to the trainable parameters. Since symbol detection is a classification task, we focus on $\mathcal{L}_{\mathcal{Q}^*}$ being the empirical cross-entropy loss, such that (1) approximates the

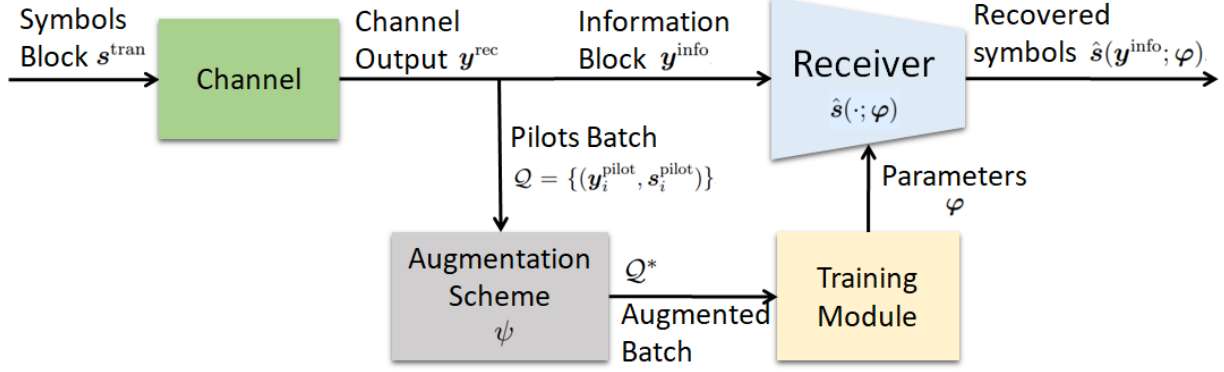


Fig. 1: DNN-aided receiver operation illustration, with the block marked with ψ representing the augmentation scheme.

solution to

$$\arg \min_{\varphi} \left\{ \mathcal{L}_{Q^*}(\varphi) = - \sum_{(\mathbf{y}_i, \mathbf{s}_i) \in Q^*} \log \hat{P}_{\varphi}(\mathbf{s}_i | \mathbf{y}_i) \right\}, \quad (2)$$

with $\hat{P}_{\varphi}(\cdot | \cdot)$ representing the soft (probabilistic) estimates produced by the receiver with DNN parameters φ .

While the DNN-aided receiver trains with a labeled data set for which the transmitted symbols are known, its performance is measured in its ability to recover the information data from the known constellation \mathcal{S} . Consequently, the considered performance measure for evaluating the parameters φ trained via (1) is the bit error rate (BER) over the information block, given by

$$e(\varphi) = \frac{1}{B^{\text{info}}} \sum_{i=B^{\text{pilot}}+1}^{B^{\text{tran}}} \Pr(\hat{\mathbf{s}}_i(\mathbf{y}^{\text{info}}; \varphi) \neq \mathbf{s}_i^{\text{info}}). \quad (3)$$

An illustration of the system is depicted in Fig. 1.

C. Problem Formulation

The labeled data set corresponding to the current channel to which the receiver has access is given by $\mathcal{Q} = \{(\mathbf{y}_i^{\text{pilot}}, \mathbf{s}_i^{\text{pilot}}) | i \in \{1, 2, \dots, B^{\text{pilot}}\}\}$, i.e., the known pilots and their respective received values. When the number of samples B^{pilot} is relatively small, training via (1) with the data set $\mathcal{Q}^* = \mathcal{Q}$ is likely to result in poor information error rates. Consequently, we opt to augment new data for training.

Our goal is to derive an augmentation scheme $\psi : \mathcal{Q} \mapsto \mathcal{Q}^*$ that enriches the available data \mathcal{Q} into the training set \mathcal{Q}^* . In particular, after training with \mathcal{Q}^* , one should result in parameters

φ that improve upon training with \mathcal{Q} in the sense of the BER objective (3). The integration of data augmentation into the overall receiver operation is illustrated in the bottom part of Fig. 1.

III. DATA AUGMENTATIONS FOR STATIC CHANNELS

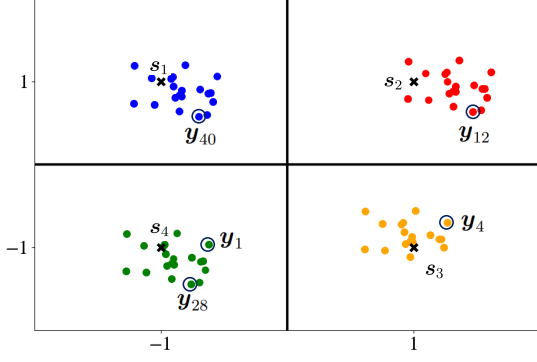
Here, we present the proposed data augmentation techniques, considering a static setting, in which one has access to a small data set corresponding to a single channel realization where it should also infer. In Subsection III-A we introduce the rationale for using augmentations, and discuss the main pillars for data augmentation techniques in light of the operation of DNN-aided communication receivers. We follow up with the communication-oriented augmentations in Subsection III-B, and provide a discussion in Subsection III-C.

A. Rationale

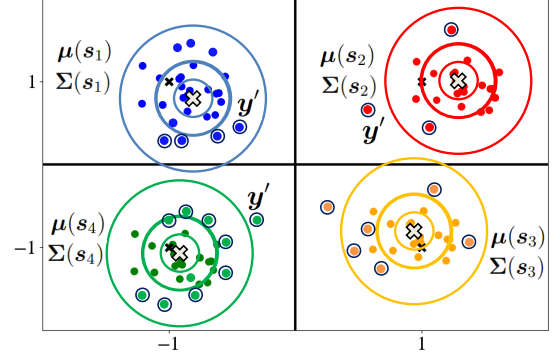
Data augmentation is a widely-spread practice in machine learning. For example, in speech processing, data augmentation includes several domain-tailored transforms such as time warping and frequency masking [40], which use observed sequences to generate new sequences that the system should learn to cope with. In general, the purpose of using augmentations is to enrich a data set by exploiting domain knowledge regarding the nature of the data, and by doing so, encourage the trainable model to learn some known property of the data. The enriched set is then used for training the model with samples that may be observed during inference, but are not included in the original training set.

In digital communications, one is often faced with scarce data scenarios corresponding to a given task, and thus augmentations can aid in obtaining new data for training DNN-aided receivers. However, existing data augmentation techniques are highly geared towards structures and invariances exhibited by data in conventional machine learning domains such as visual, language, and speech data, and thus cannot be directly implemented in digital communications. Therefore, in the following sections, we develop augmentation techniques for data used by digital receivers. Our approach accounts for the following data augmentation considerations:

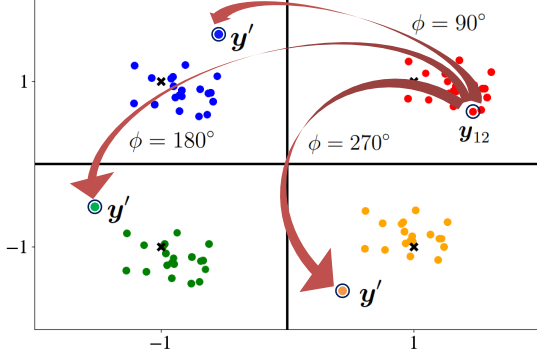
- C1 Domain-oriented** - Data augmentations are inherently domain-oriented [42]. In our case, we exploit the inherent structure of digital constellations, e.g., that some specific rotations applied to constellation symbols yield other valid symbols, to formulate constellation-preserving transformations.
- C2 Diversity** - The number of classes grows quickly with the system parameters such as the constellation size and the number of users. As such, the number of samples per class



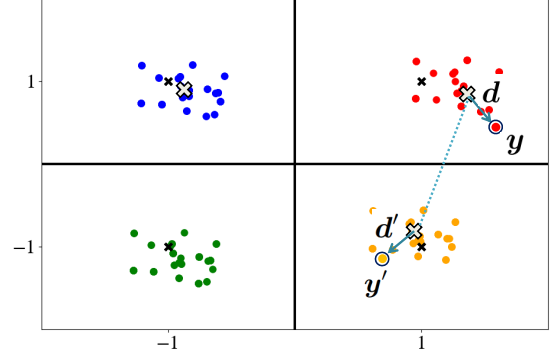
(a) Constellation points and received pilots



(b) Geometric augmentation



(c) Constellation-conserving rotation



(d) Translation augmentation

Fig. 2: Augmentations exemplified on QPSK constellation

should be kept above some minimal threshold to avoid class imbalances [35], [36], [43]. Our devised augmentations should suffice this threshold.

C3 Complexity - As our proposed data augmentation is to be implemented by a digital receiver in real-time, we must keep the sample-complexity low and the computation lightweight. This limits the usage of data augmentation approaches based on additional generative DNNs, commonly considered in conventional deep learning domains¹ [45], [46], and motivates us to focus on simpler augmentation methods based on geometric considerations and class translations.

¹For example, in [44], the authors note that "The high computational complexity (of generative models) makes it difficult to deploy state-of-the-art generative models to edge devices."

B. Augmentations

Designing data augmentations requires one to identify label-invariant transformations that account for some knowledge about the statistical model of data. For DNN-aided digital receivers, this statistical model is the underlying input-output relationship induced by the communication channel. In the following, we detail three different and complementary augmentations: (1) geometric augmentation; (2) constellation-preserving projection; and (3) translation augmentation. Each of these methods originates from some expected behaviour of wireless communications channels.

1) Geometric Augmentation: Our first augmentation technique draws inspiration from the common model of wireless channels as being decomposable into a channel response and an additive noise term. In such cases, one can write

$$\mathbf{y} = g(\mathbf{s}) + \mathbf{n}, \quad (4)$$

where g is the channel input-to-output transformation, and \mathbf{n} is an additive distortion term which is independent of \mathbf{s} , e.g., thermal noise and interference. This representation indicates that channel outputs corresponding to the same input tend to form clusters, as illustrated in Fig. 2a, where the intra-cluster distribution is invariant of the center, since the noise is independent of the signal. This geometrical interpretation of the by-class clusters can be employed to generate additional class-specific data.

In particular, we propose to use the existing labeled data \mathcal{Q} to identify clusters in the observations space from which the received symbols are likely to originate. Our method is based on clustering the channel outputs in \mathcal{Q} and setting $\boldsymbol{\mu}$ and $\boldsymbol{\Sigma}$ to be the cluster-wise centers and covariances, respectively. Using the identified clusters, we suggest to synthesize data corresponding to a constellation point \mathbf{s} from a conditional Gaussian distribution $\mathcal{N}(\boldsymbol{\mu}(\mathbf{s}), \boldsymbol{\Sigma}(\mathbf{s}))$.

Therefore, in order to enrich a labeled data set \mathcal{Q} into \mathcal{Q}^* , we use \mathcal{Q} to determine $\boldsymbol{\mu}$ and $\boldsymbol{\Sigma}$ for each $\mathbf{s} \in \mathcal{S}$. To that aim, we define the index set corresponding to \mathbf{s} as

$$\mathcal{I}_{\mathcal{Q}}(\mathbf{s}) := \{i | \mathbf{s}_i \in \mathcal{Q}; \mathbf{s}_i = \mathbf{s}\}. \quad (5)$$

We can now estimate the moments of the clusters as

$$\boldsymbol{\mu}(\mathbf{s}) = \frac{1}{|\mathcal{I}_{\mathcal{Q}}(\mathbf{s})|} \sum_{\mathbf{y}_i \in \mathcal{Q}; i \in \mathcal{I}_{\mathcal{Q}}(\mathbf{s})} \mathbf{y}_i, \quad (6)$$

and similarly

$$\Sigma(\mathbf{s}) = \frac{1}{|\mathcal{I}_Q(\mathbf{s})|} \sum_{\mathbf{y}_i \in Q: i \in \mathcal{I}_Q(\mathbf{s})} (\mathbf{y}_i - \boldsymbol{\mu}(\mathbf{s}))(\mathbf{y}_i - \boldsymbol{\mu}(\mathbf{s}))^H. \quad (7)$$

To avoid empty sets $\mathcal{I}(\mathbf{s})$, the pilot sequences should preferably be designed such that each class has at least a single representative. The augmentation is depicted in Fig. 2b. Once the clusters are estimated, they are used to draw synthetic samples \mathbf{y}' for some corresponding label \mathbf{s}' . We generate these synthetic samples from the conditional distribution $\mathcal{N}(\boldsymbol{\mu}(\mathbf{s}), \Sigma(\mathbf{s}))$.

2) *Constellation-Conserving Projections*: Many digital constellations, including phase shift keying and quadrature amplitude modulation, are symmetric by design. This means that there exists a discrete set of linear projections $\{\mathbf{P}^{\text{cc}}\}$ which are *constellation-conserving*. A matrix \mathbf{P}^{cc} , with size of $K \times K$, represents a constellation-conserving projection if for every $\mathbf{s} \in \mathcal{S}$, it is satisfied that $\mathbf{P}^{\text{cc}}\mathbf{s} \in \mathcal{S}$ as well. This property may be exploited to generate additional training data when the underlying channel meets the following two requirements:

- There exists an $N \times N$ matrix $\tilde{\mathbf{P}}^{\text{cc}}$ such that the channel mapping $g(\cdot)$ in (4) (approximately) satisfies $\tilde{\mathbf{P}}^{\text{cc}}g(\mathbf{s}) \approx g(\mathbf{P}^{\text{cc}}\mathbf{s})$.
- The distribution of the noise \mathbf{n} in (4) is invariant to the transformation, i.e., that $\mathbf{n}^{\text{cc}} = \tilde{\mathbf{P}}^{\text{cc}}\mathbf{n}$ obeys (approximately) the same distribution as \mathbf{n} .

When the above hold, one can use a labeled pair (\mathbf{y}, \mathbf{s}) to generate additional data $(\mathbf{y}', \mathbf{s}')$ by rotating the channel output. This follows since there exists $\mathbf{s}' \in \mathcal{S}$ such that

$$\begin{aligned} \mathbf{y}' &= \tilde{\mathbf{P}}^{\text{cc}}\mathbf{y} = \tilde{\mathbf{P}}^{\text{cc}}g(\mathbf{s}) + \tilde{\mathbf{P}}^{\text{cc}}\mathbf{n} \\ &\approx g(\mathbf{P}^{\text{cc}}\mathbf{s}) + \mathbf{n}^{\text{cc}} = g(\mathbf{s}') + \mathbf{n}^{\text{cc}}. \end{aligned} \quad (8)$$

The joint distribution of $\mathbf{s}' = \mathbf{P}^{\text{cc}}\mathbf{s}$ and \mathbf{y}' in (8) is (approximately) identical to that of (\mathbf{y}, \mathbf{s}) .

To design constellation-preserving augmentations, we note that communication channel mappings are often commutative to scalar multiplication, i.e., $g(a\mathbf{s}) = ag(\mathbf{s})$ for scalar a . This holds for instance, when the channel is linear or piecewise linear. Consequently, we suggest to utilize discrete rotations transformations, for which $\mathbf{P}^{\text{cc}} = e^{j\phi}\mathbf{I}_K$ and $\tilde{\mathbf{P}}^{\text{cc}} = e^{j\phi}\mathbf{I}_N$ where $\phi \in [0, 2\pi)$. For example, under a quadrature phase shift keying (QPSK) constellation ($M = 4$), one can set $\phi = \frac{\pi m}{2}$ for any $m \in \{0, 1, 2, 3\}$ such that $\mathbf{P}^{\text{cc}}\mathbf{s}$ is a valid constellation point. Furthermore, the distribution of noise signals is often well-approximated as being rotation-invariant, as is the case for, e.g., circularly-symmetric Gaussian \mathbf{n} . Consequently, applying these permutations is likely

to be constellation-preserving and satisfy the above requirements.

The resulting proposed augmentation operates by randomly choosing \mathbf{P}^{cc} out of the set of constellation preserving rotations $\{e^{j\phi}\mathbf{I}\}$, and applying it to a labeled sample in \mathcal{Q} :

$$\mathbf{y}' = \tilde{\mathbf{P}}^{\text{cc}}\mathbf{y}, \quad \mathbf{s}' = \mathbf{P}^{\text{cc}}\mathbf{s}. \quad (9)$$

The augmented pair $(\mathbf{y}', \mathbf{s}')$ is added to the buffer \mathcal{Q}^* . An illustration of the generation of such a synthetic example is depicted in Fig. 2c.

3) *Translation Augmentation*: We further exploit the idea of projections to share and exploit data from different clusters, by *translation* of samples across the clusters. Here, we again build upon the additive distortion model in (4), but instead of generating new samples around a given cluster in a random fashion, we synthesize a new *realization* of the distortion, which is used together with the cluster center to create a new observation.

To formulate this idea, let $\boldsymbol{\mu}(s)$ be the cluster center estimated in (6), and \mathbf{d} be the empirical difference vector estimated as

$$\mathbf{d} = \mathbf{y} - \boldsymbol{\mu}(s). \quad (10)$$

We aim to translate a known realization \mathbf{d} across different clusters via a translation operation defined via the $N \times N$ translation matrix \mathbf{P}^{tr} , such that $\mathbf{d}' = \mathbf{P}^{\text{tr}}\mathbf{d}$. Specifically, to generate a labeled augmented pair $(\mathbf{y}', \mathbf{s}')$ from a given (\mathbf{y}, s) , we first compute \mathbf{d} via (10). Then, we select $\mathbf{s}' \neq s$, and generate a synthetic channel output via:

$$\begin{aligned} \mathbf{y}' &= \boldsymbol{\mu}(s') + \mathbf{d}' = \boldsymbol{\mu}(s') + \mathbf{P}^{\text{tr}}\mathbf{d} \\ &= \mathbf{P}^{\text{tr}}\mathbf{y} + \boldsymbol{\mu}(s') - \mathbf{P}^{\text{tr}}\boldsymbol{\mu}(s). \end{aligned} \quad (11)$$

Now, by introducing the notation $\Delta = \boldsymbol{\mu}(s') - \mathbf{P}^{\text{tr}}\boldsymbol{\mu}(s)$, we obtain the synthetic channel output \mathbf{y}' as

$$\mathbf{y}' = \mathbf{P}^{\text{tr}}\mathbf{y} + \Delta \quad (12)$$

and the augmented pair $(\mathbf{y}', \mathbf{s}')$ is added to the buffer \mathcal{Q}^* .

The selection of the translation matrix \mathbf{P}^{tr} captures the differences between the distortion realizations added for different symbols. Since the magnitude of the distortion is often invariant to the transmitted symbols, we opt unitary translation matrices. In particular, for the sake of simplicity, we employ discrete rotations transformations here as in the constellation-conserving

projections case, for which $\mathbf{P}^{\text{tr}} = e^{j\phi} \mathbf{I}_N$ where $\phi \in [0, 2\pi)$. For example, under QPSK constellation ($M = 4$), one can set $\phi = \frac{\pi m}{2}$ for any $m \in \{0, 1, 2, 3\}$.

As opposed to the geometric augmentation approach described above, translation augmentation does not impose a statistical model on the distortion for generating new samples. Instead, it re-uses observed realizations of the distortion term of a sample in some class for augmenting samples in other classes.

4) *Combined Scheme*: Each of the aforementioned methods allows to generate additional new data from an available labeled set comprised of channel outputs and their corresponding transmitted symbols. As these methods are complementary of each other, we combine them into an overall data augmentation method by applying them subsequently.

First, we initialize the buffer containing the data to be used for training using the available limited set, i.e., by setting $\mathcal{Q}^* = \mathcal{Q}$. To realize the diversity consideration **C2**, we augment each sample into κ new samples using any combination of the above techniques. All synthetic samples are added to the augmented training batch \mathcal{Q}^* . When all three augmentations are used, this results in a set of $|\mathcal{Q}^*| = (3\kappa + 1) \cdot |\mathcal{Q}|$ labeled samples to be used for training φ , as illustrated in Fig. 1. Note the each augmentation may be applied on its own, or in consecutive pairs. However, we provide empirical demonstration in Subsection **V-G** that augmented pairs which are the output of two different augmentations are often approximately independent of each other, causing the gain from each augmentation to sum up. The resulting combined augmentation policy $\psi_{\text{static}} : \mathcal{Q} \mapsto \mathcal{Q}^*$ for static channels, combining all of the aforementioned techniques sequentially, is formulated in full as Algorithm 1.

C. Discussion

Algorithm 1 integrates data augmentation into digital receiver processing, synthesizing channel outputs data from knowledge of the constellation and the available pilots. This augmented data set allows the receiver to train without relying on lengthy pilot transmissions, achieving accurate training with short pilots as empirically demonstrated in Section **V**. The suggested policy differs from augmentations in other domains, e.g., vision, being specifically tailored to communications. The domain knowledge leveraged in our design includes the geometric interpretation of the channel outputs which follows from the typical arrangements of digital constellations; the symmetry of common digital constellations; and the expected symbol diversity, as digital receivers are likely to observe some minimal amount of all possible communication symbols.

Algorithm 1: Static Channel Augmentation Scheme ψ_{static}

Input : data set \mathcal{Q} ;
 augmentation factor κ

```
1 Augmentation Scheme ( $\mathcal{Q}, \kappa$ )
2    $\mu(\mathbf{s}) \leftarrow$  calculate by (6),  $\forall \mathbf{s} \in \mathcal{S}$ ;
3    $\Sigma(\mathbf{s}) \leftarrow$  calculate by (7),  $\forall \mathbf{s} \in \mathcal{S}$ ;
4    $\mathcal{D} \leftarrow$  calculate by (10),  $\forall (\mathbf{y}_i^{\text{pilot}}, \mathbf{s}_i^{\text{pilot}}) \in \mathcal{Q}$ ;
5   Initialize  $\mathcal{Q}^* = \mathcal{Q}$ ;
6   repeat  $\kappa$  times
7     for  $(\mathbf{y}_i, \mathbf{s}_i)$  in  $\mathcal{Q}$  do
8       Geometric Augmentation;
9       sample  $\mathbf{y}'_i$  from  $\mathcal{N}(\mu(\mathbf{s}_i), \Sigma(\mathbf{s}_i))$ ;
10      add  $(\mathbf{y}'_i, \mathbf{s}_i)$  to buffer  $\mathcal{Q}^*$ ;
11      Constellation-Conserving Projection;
12      choose a random  $\mathbf{P}^{\text{cc}}$  and its corresponding  $\tilde{\mathbf{P}}^{\text{cc}}$ ;
13       $\mathbf{y}''_i, \mathbf{s}''_i \leftarrow$  projection from  $\mathbf{y}_i, \mathbf{s}_i$  using  $\mathbf{P}^{\text{cc}}$  and  $\tilde{\mathbf{P}}^{\text{cc}}$  by (9);
14      add  $(\mathbf{y}''_i, \mathbf{s}''_i)$  to buffer  $\mathcal{Q}^*$ ;
15      Translation Augmentation;
16      choose a  $\mathbf{P}^{\text{tr}}$  and a random  $\mathbf{s}'''_i \neq \mathbf{s}_i$ ;
17       $\Delta \leftarrow \mu(\mathbf{s}'''_i) - \mathbf{P}^{\text{tr}} \mu(\mathbf{s}_i)$ ;
18       $\mathbf{y}'''_i \leftarrow$  calculate from  $\mathbf{y}_i, \Delta$  and  $\mathbf{P}^{\text{tr}}$  by (12);
19      add  $(\mathbf{y}'''_i, \mathbf{s}'''_i)$  to buffer  $\mathcal{Q}^*$ ;
20   end
21 end
22 return  $\mathcal{Q}^*$ 
```

Contrary to other domains, where augmentations often rely on complex policies, e.g., using generative networks [45] or reinforcement learning [46], we keep our mechanism light. The operations required for our scheme include sampling from a Gaussian distribution, adding and subtracting vectors, and multiplying by a scalar phase. These operations allow our mechanism to be carried out in real time. In the following section we show how one can also incorporate knowledge regarding the continuous operation of digital receivers, which allows to benefit from data corresponding to past channels, while still restricting the framework to simple computations.

Algorithm 1 can be combined with other approaches for training deep receivers with scarce data. These approaches include the usage of model-based architectures that support the usage of compact DNNs [5], [8], as well as self-supervision methods [23], [36], which assign decision-directed labels to channel outputs and uses them for training. While self-supervision cannot generate more samples than the block length, Algorithm 1 can synthesize any number of samples, and is thus suitable for coping with short block lengths.

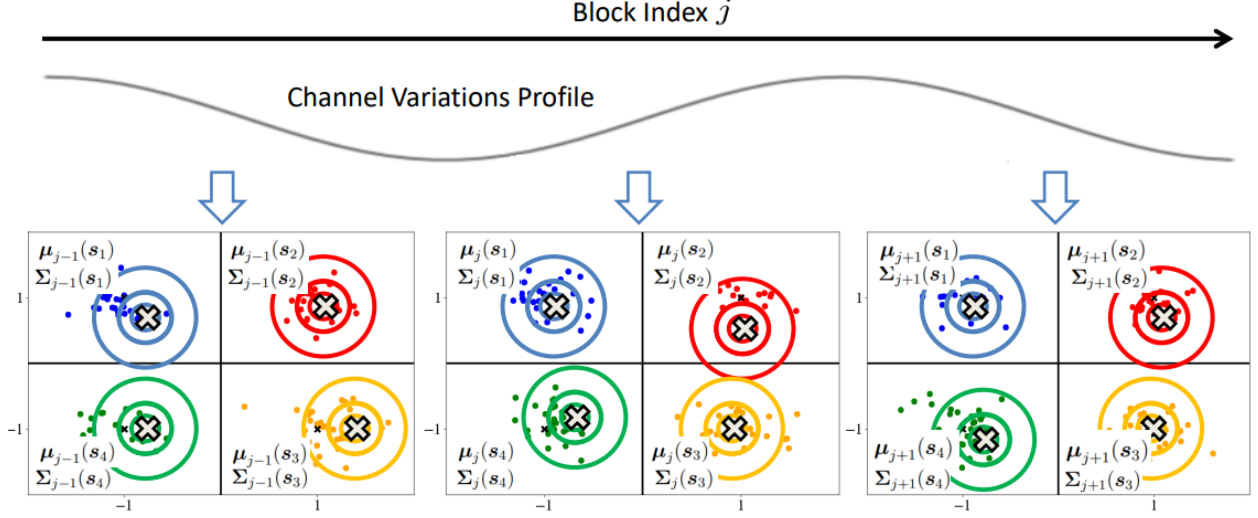


Fig. 3: Time-varying channels may benefit from an adaptive augmentation scheme.

IV. DATA AUGMENTATIONS FOR DYNAMIC CHANNELS

A. Rationale

Often in practice, digital receivers operate in block-fading channel conditions. In such cases, each block of B symbols undergoes a different channel. To formulate this, in the sequel we add a subscript j representing the block index, where the block-fading property implies that the statistical relationship between the channel outputs at the j th block $\{\mathbf{y}_{i,j}\}_{i=1}^B$ and the symbols $\{\mathbf{s}_{i,j}\}_{i=1}^B$ varies with j .

While each block requires a different receiver mapping φ_j , the data augmentation scheme ψ can possibly tune itself between different realizations. For such settings, we are interested in data augmentation schemes that are *adaptive*, and are capable of leveraging past channel realizations to improve their ability to synthesize useful training data \mathcal{Q}_j^* from the current pilots, as illustrated in Fig. 3. Since in this section the proposed scheme is adaptive, the mapping ψ depends not only on the available data \mathcal{Q}_j , but also on the previously used augmentation, i.e., the mapping applied in the previous block for block fading settings, denoted ψ_{prev} .

B. Adaptive Augmentation

The geometric and translation augmentation techniques proposed in the previous section for static channels both rely on the formulation of clusters, that are used for generating additional synthetic data. In block-fading settings, we propose to adaptively smooth the estimated clusters parameters (6) and (7) via a windowed smoothing approach. This way, we combine data across multiple time frames, while reducing the effect of outliers and burst noise during pilot signaling

Algorithm 2: Dynamic Channel Augmentation Scheme ψ_{static} at block j

Input : data set from current block \mathcal{Q}_j ; previous augmentation ψ_{prev}
augmentation factor κ ; Smoothing hyperparameters α_1, α_2

- 1 **Augmentation Scheme** ($\mathcal{Q}_j, \psi_{\text{prev}}, \kappa, \alpha_1, \alpha_2$)
 - 2 $\boldsymbol{\mu}_j(\mathbf{s}) \leftarrow$ calculate by (13), $\forall \mathbf{s} \in \mathcal{S}$;
 - 3 $\boldsymbol{\Sigma}_j(\mathbf{s}) \leftarrow$ calculate by (14), $\forall \mathbf{s} \in \mathcal{S}$;
 - 4 **apply steps 4-18 of Algorithm 1** ;
 - 5 **return** \mathcal{Q}_j^*
-

on the estimated clusters, which in turn degrades the usefulness of samples generated from these clusters.

In particular, the motivation stems from the fact that adjacent blocks may have different number of samples per class in each block, which induces high-variance noise in the estimates of the first and second order statistical moments of the classes. To reduce the noise effects, we exploit the two key properties of digital communications in time-varying channels:

- 1) DNN-aided receivers operate over multiple channel realization, and have thus observed data corresponding to past channel realizations.
- 2) The variations observed in communication channels are often of a continuous nature.

Based on the above, we make the augmentation scheme adaptive by incorporating adaptive smoothing. At block index j , the clustering mapping utilized by ψ_{prev} , denoted $\boldsymbol{\mu}_{j-1}(\cdot)$, and $\boldsymbol{\Sigma}_{j-1}(\cdot)$, is accounted for when updating the current clustering via

$$\boldsymbol{\mu}_j(\mathbf{s}) = \frac{\alpha_1}{|\mathcal{I}_{\mathcal{Q}_j}(\mathbf{s})|} \sum_{\mathbf{y}_{i,j} \in \mathcal{Q}_j: i \in \mathcal{I}_{\mathcal{Q}_j}(\mathbf{s})} \mathbf{y}_{i,j} + (1 - \alpha_1) \cdot \boldsymbol{\mu}_{j-1}(\mathbf{s}), \quad (13)$$

and

$$\boldsymbol{\Sigma}_j(\mathbf{s}) = \frac{\alpha_2}{|\mathcal{I}_{\mathcal{Q}_j}(\mathbf{s})|} \sum_{\mathbf{y}_{i,j} \in \mathcal{Q}_j: i \in \mathcal{I}_{\mathcal{Q}_j}(\mathbf{s})} (\mathbf{y}_{i,j} - \boldsymbol{\mu}_j(\mathbf{s}))(\mathbf{y}_{i,j} - \boldsymbol{\mu}_j(\mathbf{s}))^H + (1 - \alpha_2) \cdot \boldsymbol{\Sigma}_{j-1}(\mathbf{s}). \quad (14)$$

Here, $\alpha_1, \alpha_2 \in [0, 1]$ are hyperparameters balancing the contribution of ψ_{prev} on ψ . For $\alpha_1 = \alpha_2 = 1$, ψ is not adaptive and is determined solely by \mathcal{Q}_j , while for $\alpha_1 = \alpha_2 = 0$, we have $\psi \equiv \psi_{\text{prev}}$.

The dynamic channel augmentation scheme ψ_{dynamic} thus follows the same guidelines as the static augmentation design of Algorithm 1. The adaptation to temporal variations is accounted for in the estimation of the clusters by replacing lines 2 and 3 of Algorithm 1 with the calculations in (13) and (14), respectively. The resulting procedure is summarized as Algorithm 2.

V. NUMERICAL EVALUATIONS

In this section we numerically evaluate the proposed augmentation schemes ψ_{static} and ψ_{dynamic} in finite-memory SISO channels and in memoryless multi-user MIMO setups². We first describe the receivers used in our experimental study, detailing their architectures and training settings in Subsection V-A. Then, we describe the compared augmented training methods in Subsection V-B. After presenting the setup, we introduce the main simulation results for the static augmentation scheme ψ_{static} , evaluated on linear synthetic channels, in Subsection V-C. Thereafter, we present the evaluation for the dynamic augmentation scheme ψ_{dynamic} in Subsection V-D, Subsection V-E and Subsection V-F on synthetic linear channels, synthetic non-linear channels and channels obeying the COST 2100 model, respectively. Finally, we provide ablation study for the contribution of each augmentation in Subsection V-G.

A. Evaluated Receivers

The DNN-aided receiver algorithms used in our experimental study vary based on the considered settings. For each setting, we evaluate our proposed augmentations using both a black-box DNN architecture and a hybrid model-based/data-driven receiver.

1) *Finite-Memory SISO Channels*: We evaluate SISO channels, where the channel outputs are scalar, i.e., $N = 1$ with a finite memory of K samples. Here, we compare two DNN-based receivers:

- The ViterbiNet equalizer, proposed in [23], which is a DNN-based Viterbi detector [47] for finite-memory channels. ViterbiNet implements Viterbi equalization in a learned manner by computing the log likelihood metrics utilized in its internal computations using a DNN that requires no knowledge of the channel distributions. This internal DNN is implemented using three fully-connected layers of sizes 1×100 , 100×50 , and $50 \times M^K$, with activation functions set to sigmoid (after first layer), ReLU (after second layer), and softmax output layer.
- A recurrent neural network (RNN) symbol detector, comprised of a sliding-window long short-term memory (LSTM) [48] with two hidden layers of 64 cells and a window size of 1. The output of the LSTM enters a fully-connected linear layer of size $64 \times M^K$.

²The source code used in our experiments is available at <https://github.com/tomerraviv95/data-augmentations-for-receivers>.

2) *Memoryless MIMO Channels*: We evaluate two DNN-based MIMO receivers for uplink communications with K users:

- The DeepSIC receiver proposed in [22]. DeepSIC is derived from iterative soft interference cancellation (SIC) [49], which is a MIMO detection method combining multi-stage interference cancellation with soft decisions. DeepSIC here operates in 5 iterations, refining an estimate of the conditional probability mass function of each symbol based on the soft estimates of the interference symbols using a dedicated DNN. DeepSIC is thus comprised of $5K$ building block DNNs, which are implemented using three fully-connected layers: An $(N + K - 1) \times 60$ first layer, a 60×30 second layer, and a $30 \times M^K$ third layer, with a sigmoid and a ReLU intermediate activation functions, respectively.
- A black-box DNN baseline using three fully-connected layers of sizes $N \times 60$, 60×60 , and $60 \times M^K$, with ReLU activation functions in-between and softmax output layer.

All DNN-aided receivers are trained using the Adam optimizer [50] with $I_{\text{sgd}} = 500$ iterations. The learning rate for ViterbiNet and DeepSIC is set to 10^{-3} , while for the LSTM black-box and the linear fully-connected black-box it is set to 10^{-2} . Moreover, the batch size for the LSTM and the fully-connected are set to 16 and 32, respectively. These values were set empirically such that the receivers' parameters approximately converge at each time step. The complete simulation parameters can also be found in the source code that is publicly available online.

B. Augmentation Methods

As our focus is on the data used for training DNN-aided receivers, we consider the following data sets when training the aforementioned architectures:

- *Regular training*: No augmentations are applied; each receiver is trained using the original pilots batch \mathcal{Q} only.
- *Combined Scheme*: Our proposed augmentation technique ψ_{static} , which includes the sequential application of the geometric, constellation-conserving projection and translation as specified in Algorithm 1. In the case of block-fading channels, as in Subsections V-D, V-E and V-F, we apply ψ_{dynamic} (Algorithm 2) with $\alpha_1 = \alpha_2 = 0.3$.
- *Extended pilot training*: Here, no augmentations are used, however, $\beta \times B^{\text{pilot}}$ pilots are transmitted, with $\beta > 1$. Thus, the receiver has more data that is not self-generated for training compared with *Regular training*.

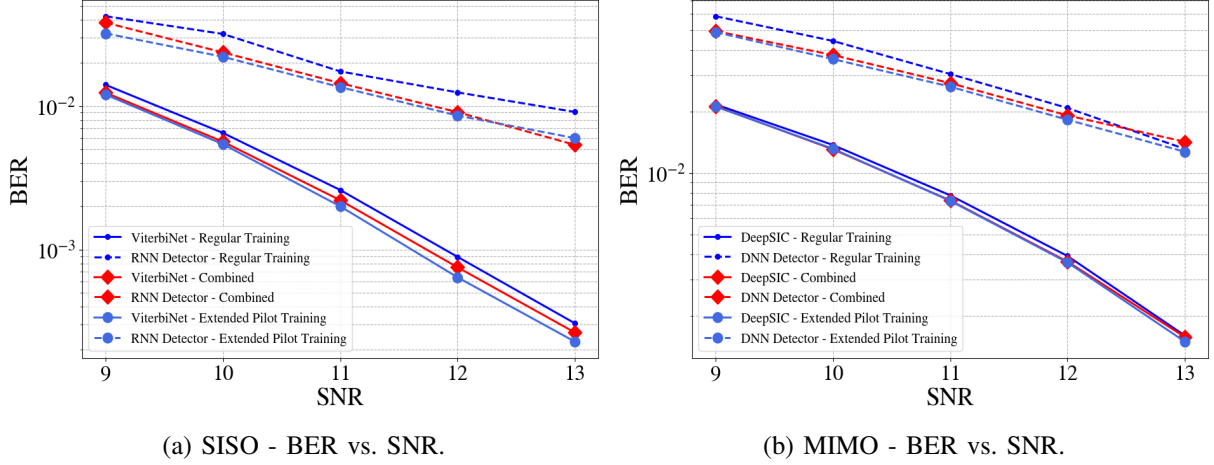


Fig. 4: Results on static synthetic linear Gaussian channel.

C. Static Linear Synthetic Channels

We begin by evaluating Algorithm 1 on stationary synthetic linear channels with additive Gaussian noise, considering a finite-memory SISO setting and a memoryless MIMO setup. As these are relatively simple settings for DNN-aided receivers, the purpose of this study is to illustrate the feasibility of the proposed augmentation and its capability of generating useful data, whose gains are further unveiled in the subsequent sections.

1) *SISO Finite-Memory Channels*: We transmit 100 blocks, each one composed of $B^{\text{pilot}} = 200$ pilots followed by $B^{\text{info}} = 10,000$ data bits, for a total transmission of a single block with size $B^{\text{tran}} = 10,200$. This means that only a small number of pilots are available to train the DNN-aided receiver. We consider a real-valued scalar linear Gaussian channel, whose input-output relationship is given by

$$y_i = \sum_{l=0}^{K-1} h_l s_{i-l} + w_i = \mathbf{h}^T \mathbf{s}_i + w_i, \quad (15)$$

where \mathbf{s}_i is the stacking of the last K channel inputs, as defined in Subsection II-A. In (15), $\mathbf{h} = [1, 0.606, 0.367, 0.223]^T$ are the real channel taps, with a channel memory of $K = 4$ and w_i is additive zero-mean white real Gaussian noise with variance σ^2 . The extended pilots method is chosen with $\beta = 2.5$, resulting in 500 total pilots, while the augmentation factor is chosen as $\kappa = 3$ for all experiments, resulting in $|\mathcal{Q}^*| = 10 \cdot |\mathcal{Q}|$.

In Fig. 4a we plot the BER evaluated via (3), averaged over the transmission of the 100 mentioned blocks, when the signal-to-noise ratio (SNR), defined as $1/\sigma^2$, takes values in the range of 9 dB - 13 dB. This figure shows that the combined augmentation approach ψ_{static}

outperforms the regular training, demonstrating gains of around 0.1 dB for the ViterbiNet (which is known to be amenable to adaptation with small training sets [23]), and up to 1 dB in the black-box RNN case. Furthermore, data augmentation allows to approach the performance achieved with extended pilots, i.e., with $2.5\times$ more pilots.

2) *Memoryless MIMO Channels:* We next consider a memoryless MIMO setting. Here, we set the number of symbols in each block to $B^{\text{pilot}} = 600$, $B^{\text{info}} = 10,000$ and $B^{\text{tran}} = 10,600$. The input-output relationship of the memoryless Gaussian MIMO channel is given by

$$\mathbf{y}_i = \mathbf{H}\mathbf{s}_i + \mathbf{w}_i, \quad (16)$$

where \mathbf{H} is a known deterministic $N \times K$ channel matrix, and \mathbf{w}_i is complex Gaussian noise with covariance $\sigma^2 \mathbf{I}_N$. We set the number of users and antennas to $K = N = 4$. The channel matrix \mathbf{H} models spatial exponential decay, and its entries are given by $(\mathbf{H})_{n,k} = e^{-|n-k|}$, for each $n \in \{1, \dots, N\}$, $k \in \{1, \dots, K\}$. The transmitted symbols are generated from a QPSK constellation in a uniform i.i.d. manner, i.e., $\mathcal{S} = \{(\pm \frac{1}{\sqrt{2}}, \pm \frac{1}{\sqrt{2}})\}^4$. Here, the extended pilot method is simulated with $\beta = 1.75$, resulting in 1,050 pilots in total, while the augmentation factor is chosen as $\kappa = 2$ for all experiments, resulting in $|\mathcal{Q}^*| = 7 \cdot |\mathcal{Q}|$.

As observed in Fig. 4b, in this synthetic setting the usage of data augmentations allows one to achieve performance similar to that of increasing the number of pilots by a factor of 1.75. In particular, since the hybrid model-based/data-driven DeepSIC only needs short pilot blocks to reliably estimate the networks' parameters under the simple synthetic linear Gaussian case [22], the addition of either augmentations or more pilots is negligible (up to 0.05 dB). For the black-box architecture which is more data-hungry, the augmentations yield gains of up to 0.5 dB, reaching close to the extended pilots baseline, in the low-to-medium SNR regime.

The above figures serve to show that our augmentations are tailored to the detection task, being agnostic to the actual structure of the receiver, and offer small but consistent improvements even in the trivial case of static linear channels.

D. Time-Varying Linear Synthetic Channels

We proceed by evaluating Algorithm 2 in block-fading synthetic linear channels with additive Gaussian noise. We again consider both the SISO or the MIMO setups. We are further interested in measuring the effective gains of our as a function of the transmitted pilots. Obviously, as the

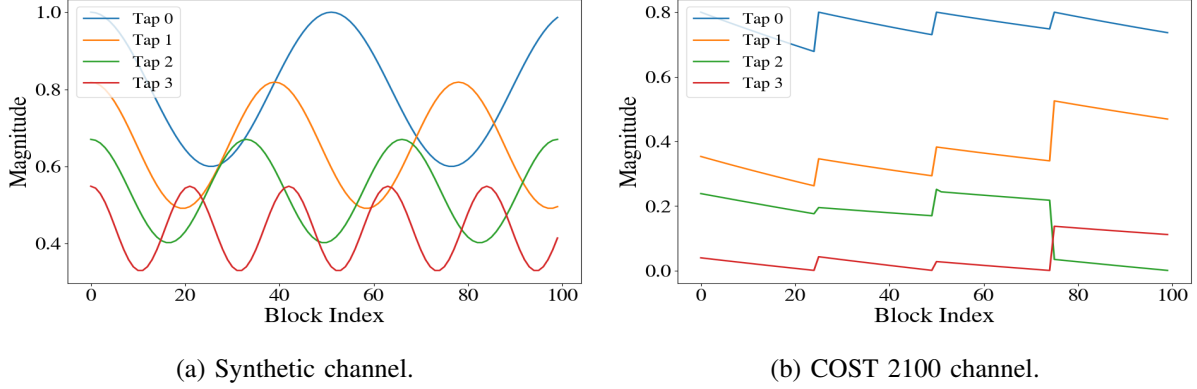


Fig. 5: Time-varying SISO channels examples: channel coefficients versus block index.

number of pilots transmitted increases, the gain of additional synthetic examples diminishes. Thus, in the following study we also quantify the effective gain of our approach.

1) *SISO Finite-Memory Channels*: We simulate a block-fading channel using the same settings of B^{pilot} , B^{info} and B^{tran} as used in Subsection V-C. For the extended pilots and combined augmentations methods, we set $\beta = 2.5$ and $\kappa = 3$. The input-output relationship is the same as in (15). Yet, here the channel taps \mathbf{h} vary between blocks following the profile depicted in Fig. 5a, which is a synthetic model representing oscillations of varying frequencies.

In Fig. 6a we plot the average BER, as in (3), for the different considered settings of \mathcal{Q}^* , when the SNR varies in the range of 9 dB - 13 dB. We observe in Fig. 6a that in the block-fading linear case, the combined approach allows the DNN-aided receivers to approach the performance achieved when training with extended pilots over all SNRs. In high SNRs, the gains increase, being significant for both the black-box RNN detector and the model-based ViterbiNet.

We next evaluate the gains in pilot efficiency, employing the proposed augmentation with $\kappa = 3$. Here, we compare the BER of the considered DNN-aided receivers for different number of pilots $|\mathcal{Q}|$ for fixed SNR of 12 dB. The results, presented in Fig. 7a, show that the proposed augmentations allow both DNN-aided receivers to improve their pilot efficiency by factors of the order of $2\times$ and $3\times$. For instance, the RNN detector requires at least 600 pilots to achieve a similar BER to that which it achieves when augmenting merely 200 pilots using the proposed method.

2) *Memoryless MIMO Channels*: For the MIMO setting, we use the same values of B^{pilot} , B^{info} , B^{tran} , β and κ , as set in Subsection V-C. The input-output relationship of the channel follows (16) with $K = N = 4$ and symbols drawn from a QPSK constellation. Here, each channel from the $K = 4$ users to one of the $N = 4$ antennas undergoes the blockwise-variations

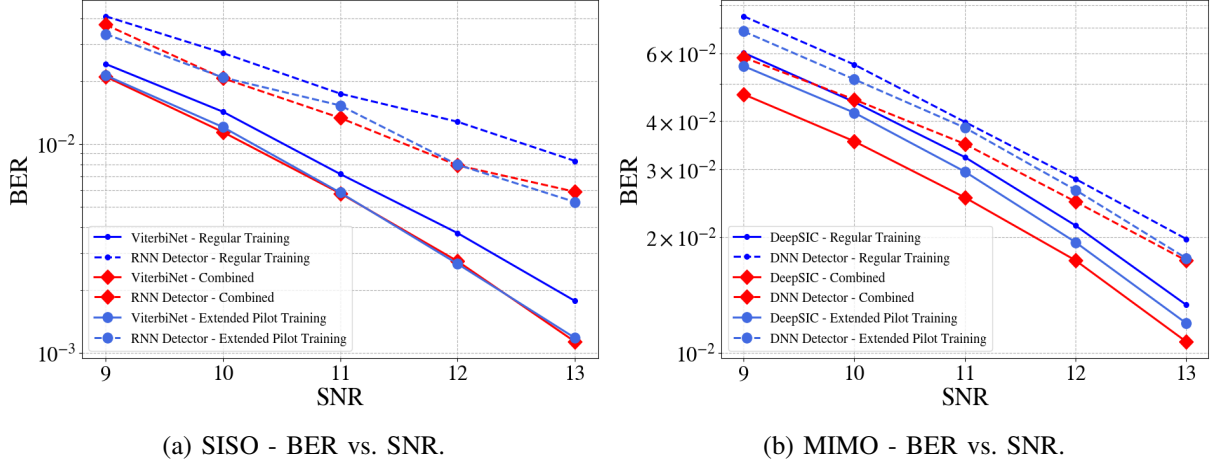
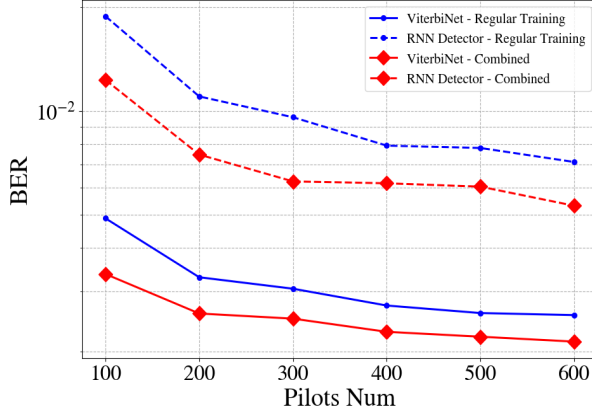


Fig. 6: Results on time-varying synthetic linear Gaussian channel.

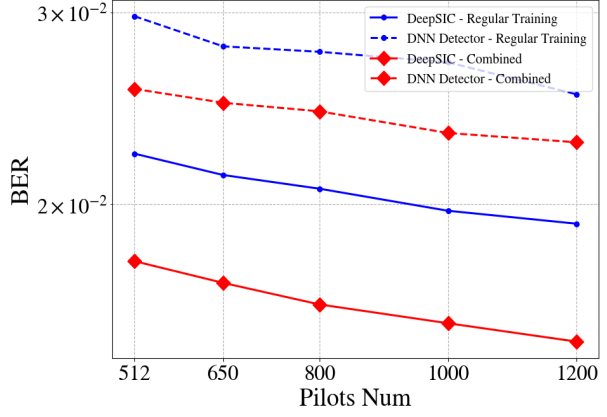
profile illustrated in Fig. 5a. This models a loss of information between each set of transmissions and the corresponding receiver in an i.i.d. manner.

As we observe in Fig. 6b, the gains of enriching a data set via the proposed augmentations here are larger than the static case. This stems from the fact that the addition of either pilots/augmentations aids in matching the momentary training distribution with the changing blockwise changes in the channel response. Both DeepSIC and the black-box DNN detector benefit from a gain of around 0.5 dB by training with our proposed augmentations scheme, over the regular training methods. The gains remain relatively consistent over all evaluated SNRs. One important highlight is that our method is able to surpass even the case of sending more pilots, as depicted by the extended pilots training method, and can thus simultaneously improve both spectral efficiency as well as BER performance.

To verify the contribution of the different augmentations on the more complex MIMO setup, we evaluate its improvements in pilot efficiency when generating data while setting $\kappa = 2$. The resulting BER versus number of pilots $|\mathcal{Q}|$ for SNR of 12 dB are reported in Fig. 7b. We observe here notable gains in pilot efficiency for both DNN-aided receivers. In particular, the BER achieved with data augmentation surpasses that of the regular training method by a factor of around $2\times$ (similar to the above SISO case) for both the model-based deep receiver and the black-box architecture. This spectral efficiency factor remains almost constant even as one increases the pilots length significantly, with no foreseeable saturation.

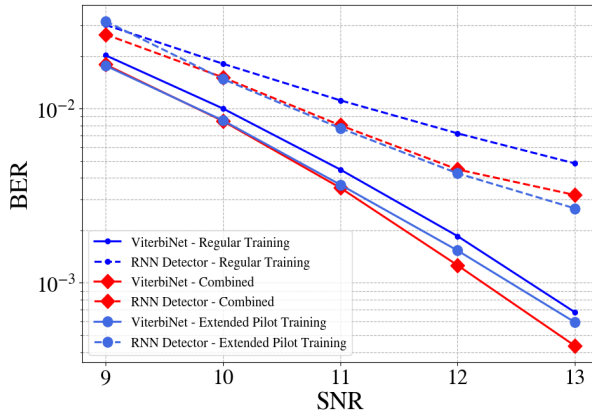


(a) SISO - BER vs. transmitted pilots.

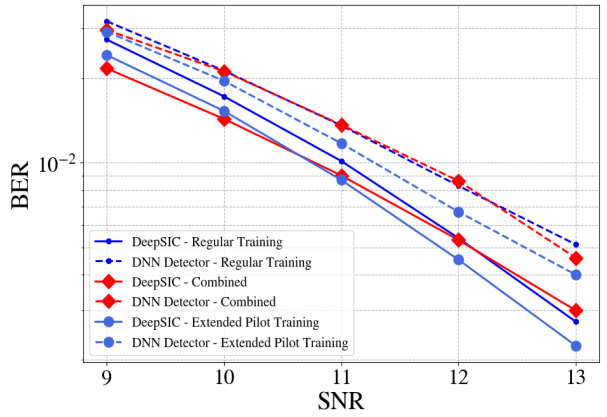


(b) MIMO - BER vs. transmitted pilots.

Fig. 7: Pilots efficiency study on time-varying synthetic linear Gaussian channel



(a) SISO - BER vs. SNR.



(b) MIMO - BER vs. SNR.

Fig. 8: Results on time-varying COST 2100 linear Gaussian channel

E. Time-Varying Linear COST Channels

Next, we evaluate the proposed augmentation scheme in time-varying linear channels, where we employ the COST 2100 model for generating the time-varying taps. The COST 2100 geometry-based stochastic channel model [51] is a widely-used model to represent wireless communications scenarios.

1) *SISO Finite-Memory Channels*: We employ a similar linear model as in 15, but incorporate a time varying characteristics:

$$y_{i,j} = \sum_{l=0}^{K-1} h_{l,j} s_{i-l,j} + w_{i,j} = \mathbf{h}_j \mathbf{s}_{i,j} + w_{i,j}. \quad (17)$$

The taps realizations $\mathbf{h}_j = [h_{0,j}, \dots, h_{K-1,j}]^T$ are generated using the wideband indoor hall 5 GHz setting of COST2100 with single-antenna elements, and $w_{i,j}$ is an additive zero-mean white

real Gaussian noise with variance σ^2 . The resulting channel taps are displayed in Fig. 5b. This setting represents a user moving in an indoor setup while switching between different microcells. Succeeding on this scenario requires high adaptivity since there is considerable mismatch in the channels observed between different blocks.

We transmit 100 blocks, and measure the average BER over all blocks and bits. The same configuration as before holds; with values of $B^{\text{pilot}} = 200$, $B^{\text{info}} = 10,000$ (that is $B^{\text{tran}} = 10,200$), $\beta = 2.5$, and $\kappa = 3$. Fig. 8a shows the average results over these 100 blocks. We observe that gains of up to 1 dB are achieved by employing our scheme, converging with the performance of the extended pilots training for the black-box architecture, while surpassing this baseline for the hybrid model-based/data-driven ViterbiNet. These gains incur only small computational cost. Specifically, they are achieved at a low cost, relying on only the simulation of additional data for training, while the same training complexity, i.e., number of iterations, is applied under each training method.

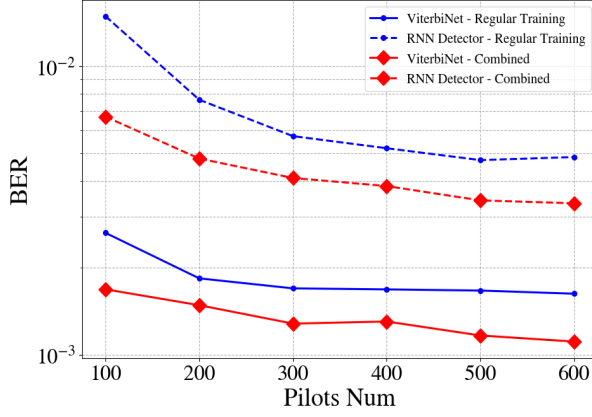
We proceed to evaluate pilot efficiency on the realistic COST channel to further validate our method. The results for SNR of 12 dB are reported in Fig. 9a, which shows that for the SISO ViterbiNet and RNN cases, the spectral efficiency factor decreases as the pilots number increases, down to a factor of $\times 2.5$ at high pilots number. That is, for $B^{\text{pilot}} = 200$, the training of the augmented versions is approximately equal to the performance achieved at $B^{\text{pilot}} = 500$ for non-augmented regular training. Moreover, while saturation is achieved quickly with the regular trained ViterbiNet architecture, the augmented training is able to further decrease the error rate with an increase of the pilots, contributing to the overall data diversity one relies on.

2) *Memoryless MIMO Channels*: Similarly to the SISO case, we simulate a time-varying linear MIMO channel from (16) via

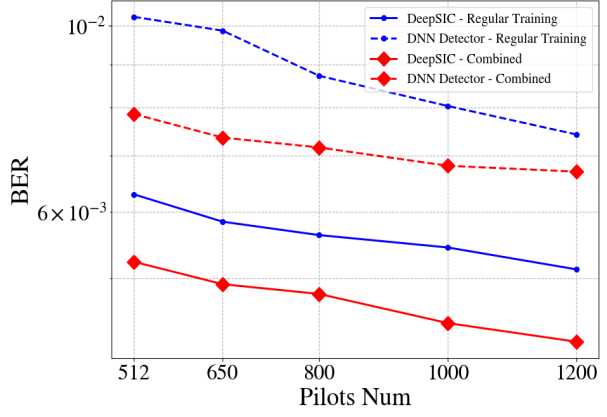
$$\mathbf{y}_{i,j} = \mathbf{H}_j \mathbf{s}_{i,j} + \mathbf{w}_{i,j}, \quad (18)$$

where the subscript j expresses the block index dependence of each term. The instantaneous channel matrix \mathbf{H}_j is simulated by following the above SISO description, and creating $4 \times 4 = 16$ narrow-band channels with COST 2100 using the 5GHz indoor configuration.

As this scenario is harder to track by any online training method, we transmit more pilots than before, setting $B^{\text{pilot}} = 1,000$, $B^{\text{info}} = 10,000$ (that is $B^{\text{tran}} = 11,000$). All other hyperparameters are as in Subsection V-C for the MIMO case. The BER results are calculated

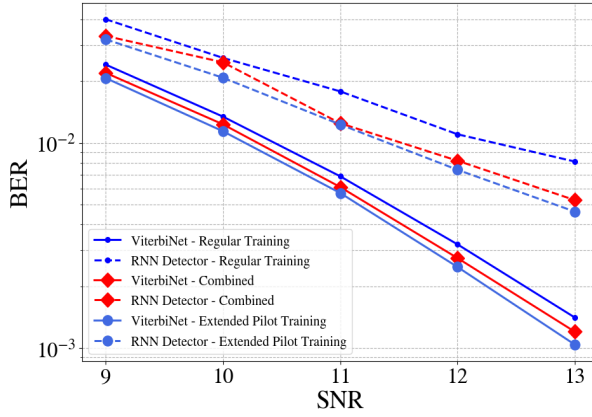


(a) SISO - BER vs. transmitted pilots.

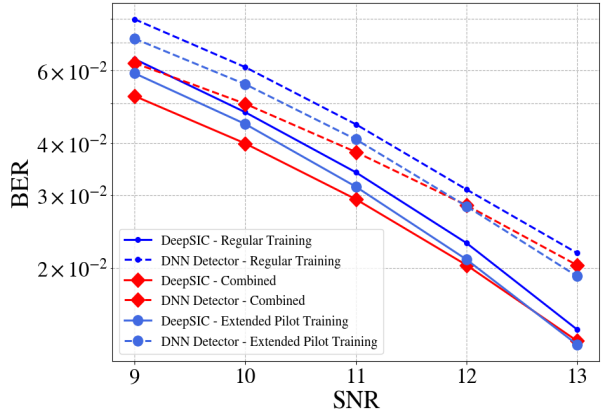


(b) MIMO - BER vs. transmitted pilots.

Fig. 9: Pilots efficiency study on time-varying COST 2100 linear Gaussian channel



(a) SISO - BER vs. SNR.



(b) MIMO - BER vs. SNR.

Fig. 10: Results on time-varying synthetic non-linear Gaussian channel

after the transmission of 100 blocks, and the resulting BER curves are reported in Fig. 8b. We observe in Fig. 8b gains of up to 0.6 dB in the low-to-medium SNR regime in the DeepSIC case, and in the high SNR regime for the black-box DNN a small gain of 0.1 dB.

To quantify the spectral efficiency gain, in Fig. 9b we observe that the BER of DeepSIC or the DNN detector trained regularly with 1200 pilot symbols is similar to the one achieved with augmented training over 650 pilot symbols only, corresponding to a gain factor of almost $\times 2$. This illustrates that our proposed augmentation is indeed beneficial on common channel models, and not only with simplistic synthetic ones.

F. Time-Varying Non-Linear Synthetic Channels

Further evaluation of the proposed online enrichment scheme is done on non-linear channels. These channels are of particular interest, as one of the motivations for DNN-based receivers arises

from the need to cope with complex channel models, as classical algorithm usually assume a linear Gaussian channel and perform rather poorly on these non-linear cases.

1) *SISO Finite-Memory Channels*: To check the robustness of our method in a non-linear case, we generate such a channel by applying a non-linear transformation to the synthetic channel in (15). The resulting finite-memory SISO channel is given by

$$y_{i,j} = \tanh \left(C \cdot \left(\sum_{l=0}^{K-1} h_{l,j} s_{i-l,j} + w_{i,j} \right) \right). \quad (19)$$

This operation may represent, e.g., non-linearities induced by the receiver acquisition hardware. The hyperparameter C stands for a power attenuation at the receiver, and was chosen empirically as $C = 1$. All other hyperparameters and settings are the same as those used in the previous subsections. The channel taps follow a fading profile as depicted in Fig. 5a.

The simulation results depicted in Fig. 10a empirically show that a consistent gain of up to 0.2 dB can be achieved by employing our scheme for the ViterbiNet receiver, or 1 dB for the black-box RNN case. Comparing with the linear case presented in Subsection V-C, we see that the overall gains by either extended pilots training, or by our proposed combined augmentations scheme, are comparable and consistent over all the SNR range.

2) *Memoryless MIMO Channels*: We simulate a non-linear MIMO channel from (16) via

$$\mathbf{y}_{i,j} = \tanh \left(C \cdot \left(\mathbf{H}_j \mathbf{s}_{i,j} + \mathbf{w}_{i,j} \right) \right), \quad (20)$$

with $C = 1$ and with simulation settings that are chosen as before in Subsection V-C. The numerical results for this channel are illustrated in Fig. 10b, showing that the superiority of our approach is maintained in non-linear setups. Compared to the linear case, we observe higher gains of up to 0.75 dB of our scheme in low-to-medium SNRs, and up to 0.2 dB in high SNRs.

G. Ablation Study of Different Augmentations

To explore how each much each augmentation contributes to the final combined approach, we next evaluate the gains achieved by the addition of each of the proposed augmentation techniques. We refer to the different augmentations proposed for static channels as *Geometric Augmentation*, *Constellation-Conserving Rotation Augmentation* and finally the *Translation Augmentation*. Each one of these augmentation techniques is compared with regular non-augmented training, as well as with the final combined approach, which employs all three augmentations sequentially as specified in Algorithm 2. We again consider both SISO and MIMO settings.

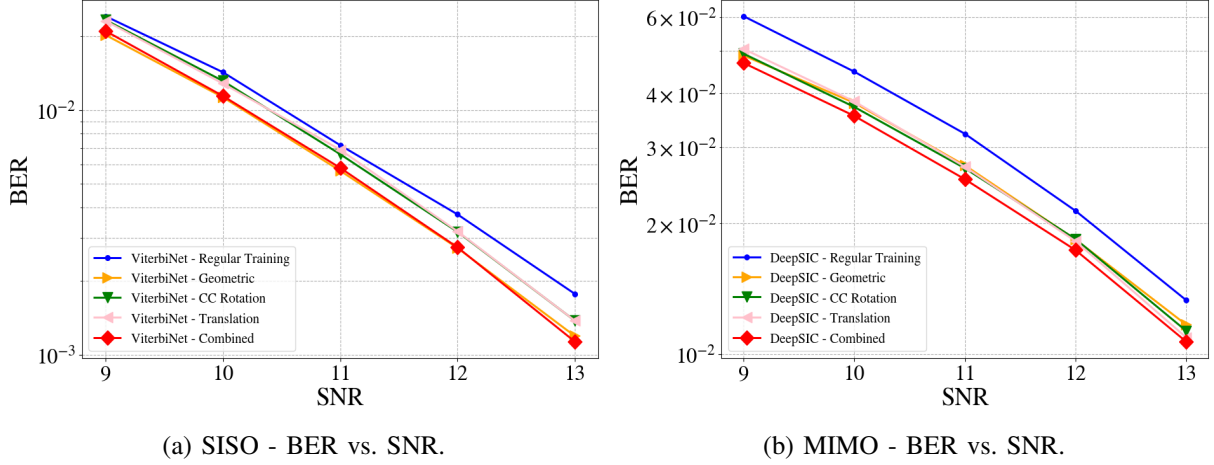


Fig. 11: Ablation study on time-varying synthetic linear Gaussian channel

1) *SISO Finite-Memory Channels*: We employ the time-varying linear synthetic channels setup from Subsection V-C, including all hyperparameters. For the single augmentation methods, we set the augmentation factor as $\kappa = 9$, resulting in $|\mathcal{Q}^*| = 10 \cdot |\mathcal{Q}|$ in total. This means that the number of samples in the single augmentation case is equal to the number of augmented samples in the combined case with $\kappa = 3$. In Fig. 11a we plot the BER versus the SNR value. It is observed in Fig. 11a that the geometric augmentation dominates over the two different ones, dictating the combined BER, up to high SNR.

2) *Memoryless MIMO Channels*: To verify the contribution of the different augmentations on the more complex MIMO setup, we again employ the time-varying linear synthetic channels setup from Subsection V-C, including all hyperparameters. The augmentation factor is chosen as $\kappa = 6$ for all single augmentation methods, again matching the number of samples in the single augmentation case to the combined augmentations approach. In Fig. 11b we observe that the BER of DeepSIC over the different augmentations surpasses that of the regular training method. Each proposed augmentation surpasses the regular training by around 0.5 dB, with the gains adding up in the combined approach, up to 0.7 dB gain over the regular training. These results demonstrate that the proposed augmentations are complementary of another, and that combining them via Algorithm 1 is indeed beneficial.

VI. CONCLUSION

In this paper, we proposed novel data augmentations techniques tailored specifically to facilitate training of DNN-aided receivers with limited data. The novelty originates from the a-priori structure of digital constellations, as well as the dynamic nature of communication channel,

which enforce the augmentations to satisfy the diversity and low complexity principles. We numerically evaluated the proposed schemes and showed that significant gains, of up to 1dB in BER and of up to $\times 3$ in spectral efficiency, can be achieved over numerous linear and non-linear scenarios via our augmentations. The synthetic pilots created aid in performance for re-training of digital receivers, while incurring only small overhead in computations (i.e. small number of additions and multiplications). Our proposed augmentations are not limited to the specific use-case, and can be further explored for other deep-learning aided communication tasks.

REFERENCES

- [1] T. Raviv and N. Shlezinger, "Adaptive data augmentation for deep receivers," in *Proc. IEEE SPAWC*, 2022.
- [2] D. Gündüz, P. de Kerret, N. D. Sidiropoulos, D. Gesbert, C. R. Murthy, and M. van der Schaar, "Machine learning in the air," *IEEE J. Sel. Areas Commun.*, vol. 37, no. 10, pp. 2184–2199, 2019.
- [3] O. Simeone, "A very brief introduction to machine learning with applications to communication systems," *IEEE Trans. on Cogn. Commun. Netw.*, vol. 4, no. 4, pp. 648–664, 2018.
- [4] A. Balatsoukas-Stimming and C. Studer, "Deep unfolding for communications systems: A survey and some new directions," *arXiv preprint arXiv:1906.05774*, 2019.
- [5] N. Farsad, N. Shlezinger, A. J. Goldsmith, and Y. C. Eldar, "Data-driven symbol detection via model-based machine learning," *arXiv preprint arXiv:2002.07806*, 2020.
- [6] W. Saad, M. Bennis, and M. Chen, "A vision of 6G wireless systems: Applications, trends, technologies, and open research problems," *IEEE Network*, vol. 34, no. 3, pp. 134–142, 2019.
- [7] N. Shlezinger, Y. C. Eldar, and S. P. Boyd, "Model-based deep learning: On the intersection of deep learning and optimization," *arXiv preprint arXiv:2205.02640*, 2022.
- [8] N. Shlezinger, J. Whang, Y. C. Eldar, and A. G. Dimakis, "Model-based deep learning," *arXiv preprint arXiv:2012.08405*, 2020.
- [9] Y. C. Eldar, A. Goldsmith, D. Gündüz, and H. V. Poor, *Machine Learning and Wireless Communications*. Cambridge University Press, 2022.
- [10] S. Cammerer, F. A. Aoudia, S. Dörner, M. Stark, J. Hoydis, and S. Ten Brink, "Trainable communication systems: Concepts and prototype," *IEEE Trans. Commun.*, vol. 68, no. 9, pp. 5489–5503, 2020.
- [11] Y. Roh, G. Heo, and S. E. Whang, "A survey on data collection for machine learning: a big data-ai integration perspective," *IEEE Trans. Knowl. Data Eng.*, vol. 33, no. 4, pp. 1328–1347, 2019.
- [12] M. Honkala, D. Korpi, and J. M. Huttunen, "DeepRx: Fully convolutional deep learning receiver," *IEEE Trans. Wireless Commun.*, vol. 20, no. 6, pp. 3925–3940, 2021.
- [13] Z. Zhao, M. C. Vuran, F. Guo, and S. D. Scott, "Deep-waveform: A learned OFDM receiver based on deep complex-valued convolutional networks," *IEEE J. Sel. Areas Commun.*, vol. 39, no. 8, pp. 2407–2420, 2021.
- [14] H. He, C.-K. Wen, S. Jin, and G. Y. Li, "Model-driven deep learning for MIMO detection," *IEEE Trans. Signal Process.*, vol. 68, pp. 1702–1715, 2020.
- [15] M. Khani, M. Alizadeh, J. Hoydis, and P. Fleming, "Adaptive neural signal detection for massive MIMO," *IEEE Trans. Wireless Commun.*, vol. 19, no. 8, pp. 5635–5648, 2020.
- [16] N. Samuel, T. Diskin, and A. Wiesel, "Learning to detect," *IEEE Trans. Signal Process.*, vol. 67, no. 10, pp. 2554–2564, 2019.

- [17] M. Goutay, F. A. Aoudia, J. Hoydis, and J.-M. Gorce, "Machine learning for MU-MIMO receive processing in OFDM systems," *IEEE J. Sel. Areas Commun.*, vol. 39, no. 8, pp. 2318–2332, 2021.
- [18] K. Pratik, B. D. Rao, and M. Welling, "RE-MIMO: Recurrent and permutation equivariant neural MIMO detection," *IEEE Trans. Signal Process.*, vol. 69, pp. 459–473, 2020.
- [19] L. Schmid and L. Schmalen, "Neural enhancement of factor graph-based symbol detection," *arXiv preprint arXiv:2203.03333*, 2022.
- [20] S. Baumgartner, O. Lang, and M. Huemer, "A soft interference cancellation inspired neural network for SC-FDE," in *Proc. IEEE SPAWC*, 2022.
- [21] N. Shlezinger, N. Farsad, Y. C. Eldar, and A. J. Goldsmith, "Data-driven factor graphs for deep symbol detection," in *Proc. IEEE ISIT*, 2020.
- [22] N. Shlezinger, R. Fu, and Y. C. Eldar, "DeepSIC: Deep soft interference cancellation for multiuser MIMO detection," *IEEE Trans. Wireless Commun.*, vol. 20, no. 2, pp. 1349–1362, 2021.
- [23] N. Shlezinger, N. Farsad, Y. C. Eldar, and A. J. Goldsmith, "ViterbiNet: A deep learning based Viterbi algorithm for symbol detection," *IEEE Trans. Wireless Commun.*, vol. 19, no. 5, pp. 3319–3331, 2020.
- [24] T. Raviv, N. Raviv, and Y. Be'ery, "Data-driven ensembles for deep and hard-decision hybrid decoding," in *Proc. IEEE ISIT*, 2020, pp. 321–326.
- [25] T. Van Luong, N. Shlezinger, C. Xu, T. M. Hoang, Y. C. Eldar, and L. Hanzo, "Deep learning based successive interference cancellation for the non-orthogonal downlink," *IEEE Trans. Veh. Technol.*, 2022.
- [26] L. Wang, N. Shlezinger, G. C. Alexandropoulos, H. Zhang, B. Wang, and Y. C. Eldar, "Jointly learned symbol detection and signal reflection in RIS-aided multi-user MIMO systems," in *Asilomar Conference on Signals, Systems, and Computers*, 2021.
- [27] S. Park, H. Jang, O. Simeone, and J. Kang, "Learning to demodulate from few pilots via offline and online meta-learning," *IEEE Trans. Signal Process.*, vol. 69, pp. 226 – 239, 2020.
- [28] S. Park, O. Simeone, and J. Kang, "Meta-learning to communicate: Fast end-to-end training for fading channels," in *Proc. IEEE ICASSP*, 2020, pp. 5075–5079.
- [29] O. Simeone, S. Park, and J. Kang, "From learning to meta-learning: Reduced training overhead and complexity for communication systems," in *IEEE 6G Wireless Summit*, 2020.
- [30] T. Raviv, S. Park, N. Shlezinger, O. Simeone, Y. C. Eldar, and J. Kang, "Meta-ViterbiNet: Online meta-learned Viterbi equalization for non-stationary channels," in *Proc. IEEE ICC*, 2021.
- [31] T. Raviv, S. Park, O. Simeone, Y. C. Eldar, and N. Shlezinger, "Online meta-learning for hybrid model-based deep receivers," *arXiv preprint arXiv:2203.14359*, 2022.
- [32] N. Shlezinger, N. Farsad, Y. C. Eldar, and A. Goldsmith, "Learned factor graphs for inference from stationary time sequences," *IEEE Trans. Signal Process.*, vol. 70, pp. 366–380, 2021.
- [33] C.-F. Teng and Y.-L. Chen, "Syndrome enabled unsupervised learning for neural network based polar decoder and jointly optimized blind equalizer," *IEEE Trans. Emerg. Sel. Topics Circuits Syst.*, 2020.
- [34] S. Schibisch, S. Cammerer, S. Dörner, J. Hoydis, and S. ten Brink, "Online label recovery for deep learning-based communication through error correcting codes," in *Proc. IEEE ISWCS*, 2018.
- [35] I. Be'ery, N. Raviv, T. Raviv, and Y. Be'ery, "Active deep decoding of linear codes," *IEEE Trans. Commun.*, vol. 68, no. 2, pp. 728–736, 2019.
- [36] R. A. Finish, Y. Cohen, T. Raviv, and N. Shlezinger, "Symbol-level online channel tracking for deep receivers," in *Proc. IEEE ICASSP*, 2022, pp. 8897–8901.

- [37] C. Shorten and T. M. Khoshgoftaar, “A survey on image data augmentation for deep learning,” *Journal of big data*, vol. 6, no. 1, pp. 1–48, 2019.
- [38] J. Nalepa, M. Marcinkiewicz, and M. Kawulok, “Data augmentation for brain-tumor segmentation: a review,” *Frontiers in computational neuroscience*, p. 83, 2019.
- [39] S. Y. Feng, V. Gangal, J. Wei, S. Chandar, S. Vosoughi, T. Mitamura, and E. Hovy, “A survey of data augmentation approaches for nlp,” *arXiv preprint arXiv:2105.03075*, 2021.
- [40] D. S. Park, W. Chan, Y. Zhang, C.-C. Chiu, B. Zoph, E. D. Cubuk, and Q. V. Le, “SpecAugment: A simple data augmentation method for automatic speech recognition,” *arXiv preprint arXiv:1904.08779*, 2019.
- [41] S. T. Jose, S. Park, and O. Simeone, “Information-theoretic analysis of epistemic uncertainty in bayesian meta-learning,” in *International Conference on Artificial Intelligence and Statistics*. PMLR, 2022, pp. 9758–9775.
- [42] A. Nooraiepour, W. U. Bajwa, and N. B. Mandayam, “A hybrid model-based and learning-based approach for classification using limited number of training samples,” *IEEE Open Journal of Signal Processing*, vol. 3, pp. 49–70, 2021.
- [43] S. Yang, W. Xiao, M. Zhang, S. Guo, J. Zhao, and F. Shen, “Image data augmentation for deep learning: A survey,” *arXiv preprint arXiv:2204.08610*, 2022.
- [44] S. Belousov, “Mobilestylegan: A lightweight convolutional neural network for high-fidelity image synthesis,” *arXiv preprint arXiv:2104.04767*, 2021.
- [45] A. Almahairi, S. Rajeshwar, A. Sordoni, P. Bachman, and A. Courville, “Augmented CycleGAN: Learning many-to-many mappings from unpaired data,” in *International Conference on Machine Learning*. PMLR, 2018, pp. 195–204.
- [46] M. Laskin, K. Lee, A. Stooke, L. Pinto, P. Abbeel, and A. Srinivas, “Reinforcement learning with augmented data,” *Advances in Neural Information Processing Systems*, vol. 33, pp. 19 884–19 895, 2020.
- [47] A. Viterbi, “Error bounds for convolutional codes and an asymptotically optimum decoding algorithm,” *IEEE Trans. Inf. Theory*, vol. 13, no. 2, pp. 260–269, 1967.
- [48] D. Tandler, S. Dörner, S. Cammerer, and S. ten Brink, “On recurrent neural networks for sequence-based processing in communications,” in *Asilomar Conference on Signals, Systems, and Computers*, 2019, pp. 537–543.
- [49] W.-J. Choi, K.-W. Cheong, and J. M. Cioffi, “Iterative soft interference cancellation for multiple antenna systems,” in *Proc. IEEE WCNC*, 2000.
- [50] D. P. Kingma and J. Ba, “Adam: A method for stochastic optimization,” *arXiv preprint arXiv:1412.6980*, 2014.
- [51] L. Liu, C. Oestges, J. Poutanen, K. Haneda, P. Vainikainen, F. Quitin, F. Tufvesson, and P. De Doncker, “The COST 2100 MIMO channel model,” *IEEE Wireless Commun.*, vol. 19, no. 6, pp. 92–99, 2012.